Introducing Dual Functional CNT Networks into CuO Nanomicrospheres toward Superior Electrode Materials for Lithium-Ion Batteries

Shu-Fa Zheng, Jin-Song Hu, Liang-Shu Zhong, Wei-Guo Song, Li-Jun Wan,* and Yu-Guo Guo*

Beijing National Laboratory for Molecular Sciences, Institute of Chemistry, Chinese Academy of Sciences, Beijing 100080, China

Received November 29, 2007. Revised Manuscript Received March 14, 2008

An optimized nanostructure design of electrode materials for high-performance lithium-ion batteries was realized by introducing three-dimensional (3D) carbon nanotube (CNT) networks into transition metal oxide nanomicrospheres. A CuO−CNT composite was selected as a typical example of the optimized design. Self-assembled CuO and CuO−CNT nanomicrospheres have been successfully synthesized by a simple solution method and investigated with SEM, TEM, XRD, and electrochemical experiments. The CuO−CNT composite spheres exhibit remarkably enhanced cycling performance and rate performance compared with CuO spheres when being used as anode materials in lithium-ion batteries. It benefits from an as-formed 3D network of CNTs, which has dual functions, viz. a 3D current collector network and an elastic buffer.

Introduction

The use of transition metal oxides as electrode materials for next generation rechargeable lithium-ion batteries with both high energy and high power densities have been widely studied because of their high theoretical capacity, high safety, environmental benignity, low cost, etc.[1] One of the challenging issues in using them for high performance lithium-ion batteries is to tackle their poor electronic conductivities. Extensive research work has focused on enhancing electronic conduction by using carbon-coatings[2,3] or other electronically conductive additives,[4,5] or by using nanoarchitectured electrodes.[6] However, either only a limited rate performance enhancement can be achieved or, in some cases, these approaches suffer from the difficulties of mass production and achieving high energy demands. Another drawback affecting the application of transition metal oxides for lithium-ion batteries is the large volume variation during the lithium uptake/release process, which leads to severe mechanical strains and very rapid capacity decay. In this context, a great effort has been made to use nanoparticles or active/inactive nanocomposites for improving the cycle life.[5] Although the former benefits from the accommodation of the strain of lithium uptake/release, the latter can be ascribed to the inactive confining buffer.

Over the past few decades, the synthesis of inorganic hierarchical nano/microstructures with well-defined morphologies has attracted considerable attention. The structural characteristics of these materials endow them with a wide range of potential applications.[7] In particular, monodisperse hierarchical nanomicrospheres, which are self-assemblies from building blocks including nanoparticles,[8] nanorods,[9] and nanosheets[10] are of great interest for scientists because of their novel physical and chemical properties. In recent years, many methods have been used to prepare complex hierarchical nanomicrospheres, including hydrothermal methods,[9] wet chemical methods,[10] thermal reduction and oxidation process,[11] oriented aggregation,[12] self-assembly of building blocks,[8] template-assisted synthesis,[13] and template-free synthesis. Carbon nanotubes (CNTs) have high chemical stability, a high length/diameter ratio, strong mechanical strength, high activated surface area, and high conductivity and are attractive materials in energy storage devices, such as pseudocapacitors, fuel cells, and secondary batteries.[14–16] Recently, integrating CNTs into functional architectures and

* Corresponding authors. E-mail: wanlijun@iccas.ac.cn (L.-J.W.); ygguo@iccas.ac.cn (Y.-G.G.). Tel. & Fax: (86)10-62558934.

(1) Jiao, F.; Bruce, P. G. *Adv. Mater.* **2007**, *19*, 657.
(2) Derrien, G.; Hassoun, J.; Panero, S.; Scrosati, B. *Adv. Mater.* **2007**, *19*, 2336.
(3) Ng, S. H.; Wang, J. Z.; Wexler, D.; Konstantinov, K.; Guo, Z. P.; Liu, H. K. *Angew. Chem., Int. Ed.* **2006**, *45*, 6896.
(4) Kavan, L.; Exnar, I.; Cech, J.; Graetzel, M. *Chem. Mater.* **2007**, *19*, 4716.
(5) Badway, F.; Mansour, A. N.; Pereira, N.; Al-Sharab, J. F.; Cosandey, F.; Plitz, I.; Amatucci, G. G. *Chem. Mater.* **2007**, *19*, 4129.
(6) Taberna, L.; Mitra, S.; Poizot, P.; Simon, P.; Tarascon, J. M. *Nat. Mater.* **2006**, *5*, 567.
(7) Cao, A. M.; Hu, J. S.; Liang, H. P.; Wan, L. J. *Angew. Chem., Int. Ed.* **2005**, *44*, 4391.
(8) Yu, J. G.; Yu, J. C.; Zhang, L. Z.; Wang, X. C.; Wu, L. *Chem. Commun.* **2004**, 2414.
(9) Zheng, Y. H.; Cheng, Y.; Wang, Y. S.; Zhou, L. H.; Bao, F.; Jia, C. *J. Phys. Chem. B* **2006**, *110*, 8284.
(10) Cao, A. M.; Hu, J. S.; Liang, H. P.; Song, W. G.; Wan, L. J.; He, X. L.; Gao, X. G.; Xia, S. H. *J. Phys. Chem. B* **2006**, *110*, 15858.
(11) Zhang, J. T.; Liu, J. F.; Peng, Q.; Wang, X.; Li, Y. D. *Chem. Mater.* **2006**, *18*, 867.
(12) Jiang, P.; Zhou, J. J.; Fang, H. F.; Wang, C. Y.; Wang, Z. L.; Xie, S. S. *Adv. Funct. Mater.* **2007**, *17*, 1303.
(13) Caruso, F.; Caruso, R. A.; Mohwald, H. *Science* **1998**, *282*, 1111.

10.1021/cm7033855 CCC: $40.75
Published on Web 05/14/2008

composites has been an active research field.[17,18] It has also been reported that constructing three-dimensional (3D) conductive network and organic/inorganic composite materials are effective methods to improve the performance of electrode materials in lithium-ion batteries.[19,20]

As a p-type transition metal oxide with a narrow band gap (E_g = 1.2 eV), CuO has been widely exploited for diverse applications as a heterogeneous catalyst, a gas sensor, a field emission emitter, and a lithium-ion electrode material.[11,21] It is also a promising material for solar cells because of its photoconductive and photochemical properties. Therefore, the synthesis and fabrication of CuO nano/micromaterials have both fundamental and practical importance. CuO nano/microstructures with different morphologies such as nanoparticles, nanoellipsoids, nanorods, nanoneedles, nanoribbons, nanoshuttles, nanoleaves, and nanotubes have been synthesized successfully. With regard to the self-assembled complex CuO architectures, 3D peanutlike patterns,[22] pricky/layered microspheres,[23] nanodendrites,[24] nanoellipsoids, and chrysanthemum-like architectures[25] have also been obtained by various methods, including thermal decomposition of malachite, water baths, hydrothermal methods, natural oxidation processes, etc. Furthermore, Liu et al. have synthesized dandelion-like CuO hollow microspheres through a mesoscale organization of CuO nanoribbons, which is available by hydrolysis of a salt in ethanol.[26]

In this paper, we propose and realize optimized nanostructure designs of transition metal oxides for high performance lithium-ion batteries, using CuO as an example. Uniform CuO−CNT composite nanomicrospheres with 3D networks of CNTs have been synthesized by a facile, large-scale wet chemical method. The composite combines the advantages of high capacity of nanoscale active materials and manageability of microscale particles. Especially, in the composite, one end of the CNTs embeds into the CuO spheres and the other end entangles CuO nanoplates outside the microspheres to form 3D conducting networks, which not only significantly enhance the electronic conductivity of the composite material but also provide an elastic buffer for releasing the strain of CuO during lithium uptake/release process. It is because of the dual functional CNT networks that the CuO−CNT composite nanomicrospheres show much enhanced cycling performance and rate performance when being used as anode materials in lithium-ion batteries.

Experimental Section

Synthesis of CuO Nanomicrospheres and CuO−CNT Composite Nanomicrospheres. All the reagents were of analytical grade and were used as received. In a typical synthesis, 1 g of block polymer P123 was dissolved in 40 mL of milli-Q water with magnetic stirring, then 0.005 mol $Cu(NO_3)_2 \cdot 5H_2O$ was added to the solution to form a blue solution followed by addition of ammonia solution (10 mL, 25 wt %). Upon the addition of ammonia solution, the solution became dark blue. After being stirred for 1 h, the dark blue solution was then transferred into a three-necked flask. The overall mixture was then refluxed at 110 °C for 2 h, during which the dark solution turned black, indicating the products were formed. Vigorous stirring was maintained throughout the entire process. After the reaction, the solution was cooled to room temperature. The black suspension and precipitate were separated by centrifugation, washed with water and absolute alcohol three times, and then dried at 80 °C.

For CuO−CNT composite nanomicrospheres, multiwalled carbon nanotubes (MWCNTs, purchased from Shenzhen Nanotech Port Co. Ltd.) were refluxed in 6 M HNO_3 solution to remove any impurity and to oxidize the opened end of the tubes, thereby making them more dispersible in water. Twenty milligrams of CNTs was ultrasonically dispersed in 5 mL of dimethyl formamide (DMF) for 5 h, and the mixture was added to the separately prepared dark blue solution as mentioned above; the overall mixture is then treated by the same procedure as CuO nanomicrospheres.

Characterization. The morphology of the final products was characterized by scanning electron microscopy (SEM, Hitachi S-4300F) and energy-dispersive X-ray spectroscopy (EDX, Phoenix). High-resolution transmission electron microscopy (HRTEM) and corresponding selected-area electron diffraction (SAED) patterns were obtained by a JEOL 2010 TEM with an accelerating voltage of 200 kV. The samples were ultrasonically dispersed in ethanol and dropped onto the TEM grids, followed by solvent evaporation in air at room temperature. The infrared spectrum was acquired using a Bruker Tensor 27. The power X-ray diffraction (XRD) patterns were obtained by a Rigaku D/max-2500 using a Cu Kα radiation. For the XPS analysis, a Kratos AXIS 165 multitechnique electron spectrometer was used. Inductively coupled plasma-optical emission spectroscopy (ICP) was used to reveal the precise chemical composition of the CuO−CNT composite. Twenty milligrams of dried CuO−CNTs was completely dissolved in 10 mL of concentrated nitric acid by heating, and the solution was then diluted to 100 mL by DI water. The diluted solution was centrifuged to remove the insoluble CNTs residual. One milliliter of the resulting solution then was diluted by 8 mL of DI water and analyzed by ICP (Profile-ICP, Leeman). The concentration of the Cu element was 16.7 mg L^{-1}. For electrical measurements, the pellets of CuO and CuO−CNTs were prepared by pressing the powder uniaxially at 20 MPa into discs with a diameter of 10 mm and a thickness of approximately 1 mm. Impedance spectra were recorded by a PARSTAT 2273 in the frequency range of 10.0 Hz−1.0 MHz.

Electrochemical properties of the products were measured using coin and Swagelok-type cells. The working electrodes were prepared by casting a slurry consisting of 80 wt % active material, 10 wt % poly(vinylidene fluoride) (PVDF), and 10 wt % carbon black onto a copper foil. The mass of active powder in each cell is ca. 2 mg on a 0.8 cm × 0.8 cm Cu foil. A Celgard 2400 microporous polypropylene membrane was used as separator. The electrolyte

(14) Park, J. H.; Ko, J. M.; Park, O. O. *J. Electrochem. Soc.* **2003**, *150*, A864.
(15) Liao, S.; Holmes, K. A.; Tsaprailis, H.; Birss, V. I. *J. Am. Chem. Soc.* **2006**, *128*, 3504.
(16) Chen, J.; Liu, Y.; Minett, A. I.; Lynam, C.; Wang, J.; Wallace, G. G. *Chem. Mater.* **2007**, *19*, 3595.
(17) Wei, C.; Dai, L.; Roy, A.; Tolle, T. B. *J. Am. Chem. Soc.* **2006**, *128*, 1412.
(18) Wang, Y.; Lee, J. Y. *Angew. Chem., Int. Ed.* **2006**, *45*, 7039.
(19) Shu, J.; Li, H.; Yang, R. Z.; Shi, Y.; Huang, X. J. *Electrochem. Commun.* **2006**, *8*, 51.
(20) Guo, Y. G.; Hu, Y. S.; Sigle, W.; Maier, J. *Adv. Mater.* **2007**, *19*, 2087.
(21) Poizot, P.; Laruelle, S.; Grugeon, S.; Dupont, L.; Tarascon, J. M. *Nature* **2000**, *407*, 496.
(22) Zhang, L. Z.; Yu, J. C.; Xu, A. W.; Li, Q.; Kwong, K. W.; Yu, S. H. *J. Cryst. Growth* **2004**, *266*, 545.
(23) Xu, Y.; Chen, D.; Jiao, X. *J. Phys. Chem. B* **2005**, *109*, 13561.
(24) Li, S. Z.; Zhang, H.; Ji, Y. J.; Yang, D. R. *Nanotechnology* **2004**, *15*, 1428.
(25) Liu, Y.; Chu, Y.; Li, M. Y.; Li, L. L.; Dong, L. H. *J. Mater. Chem.* **2006**, *16*, 192.
(26) Liu, B.; Zeng, H. C. *J. Am. Chem. Soc.* **2004**, *126*, 8124.

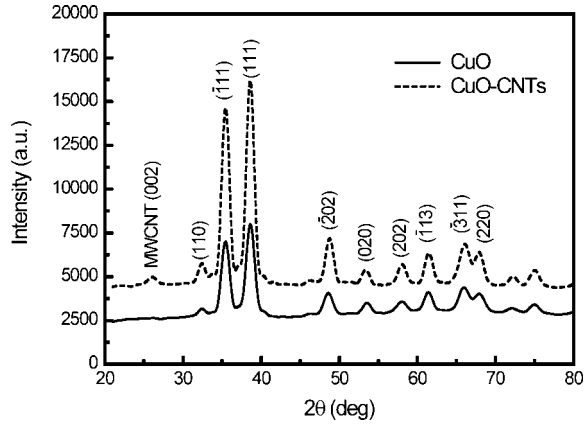

Figure 1. Typical XRD patterns of the samples: (a) CuO nanomicrospheres, (b) CuO−CNT nanomicrospheres.

consisted of a solution of 1 M LiPF6 in ethylene carbonate (EC)/dimethyl carbonate (DMC) (1:1 v/v). Lithium foil was used as counter electrodes. These cells were assembled in an argon-filled glovebox and cycled at different rates between voltage limits of 0 and 3 V. Note that we include the mass of CNTs when calculating the specific capacity of CuO−CNTs composite.

Results and Discussion

Figure 1 shows the XRD pattern of the as-prepared CuO and CuO-CNTs. All the peaks of the as-prepared CuO can be assigned to monoclinic symmetry of CuO (space group $C2/c$; $a_o = 4.684$ Å, $b_o = 3.425$ Å, $c_o = 5.129$ Å, $\beta = 99.47°$, JCPDS Card No. 05−0661).[24,26] No other peaks are observed, indicating high purity of the as-prepared samples. The broad XRD peaks also indicate the sample is composed of CuO nanocrystallines. On the other hand, the XRD pattern of the as-prepared CuO−CNTs shows an additional peak at 25° attributed to the (002) plane of hexagonal graphite structure, suggesting that the CNTs are incorporated into CuO nanomicrospheres. Furthermore, ICP was used to reveal the precise chemical composition of the composites. The results showed that the composite has a chemical composition of 94 wt % CuO and 6 wt % CNTs.

IR analysis also confirms that the as-prepared CuO samples are a pure-phase of CuO with monoclinic structure (see Figure S1 in the Supporting Information). The purity and the composition of the as-prepared CuO were further investigated by X-ray photoelectron spectroscopy (XPS, see Figure S2 in the Supporting Information). The XPS detected the Cu $2p_{3/2}$ peaks at ~934.2 eV, which is consistent with those observed in CuO.[27] The peak-fit of Cu $2p_{3/2}$ peaks revealed a main peak at 934.2 eV, which was accompanied by two satellite peaks at 941.6 and 944 eV, respectively. These features correspond to a Cu^{2+} state for Cu atoms. As shown in Figure S2b, the O 1s core-level spectrum is broad, and two Gaussian peaks (marked as I and II) were resolved by using a curve-fitting procedure. Peak I, at the lower energy of 530.1 eV, is in agreement with that for O^{2-} in CuO, while peaks II at the higher energy of 531.8 eV, is attributed to oxygen absorbed onto the surface of the CuO nanomicrospheres. The XPS results further support the conclusion that the sample is pure CuO.

The morphology of as-prepared CuO and CuO−CNT samples was examined by SEM and TEM. Images a and c in Figure 2 and Figure S3 in the Supporting Information show the typical SEM images of the as-prepared CuO sample. It can be seen that the as-prepared CuO are microspheres with an average diameter of about 2.5 μm. These microspheres are radially self-assembled by many nanoplates with a thickness of about 25 nm, which can be further confirmed from the SEM image of a broken microsphere shown in Figure 2b. It was found that P123 plays a critical role in the formation of CuO nanomicrospheres. Under the control experiment with the absence of P123, only irregular CuO nanoplates aggregations can be observed and no CuO nanomicrospheres were obtained (see panels a and b in Figure S4 in the Supporting Information). As we know, P123 is likely to form spherical micelles in solution, which can direct the growth of CuO to form nanomicrospheres and prevent the aggregation of nanoplates. The EDX spectrum shown in the inset in Figure 2c reveals that the spheres are composed of Cu and O, and quantitative analysis results indicate that the atomic ratio of Cu to O is very close to a 1:1 stoichiometry. The minor Pt peak arises from the sputtered platinum to enhancing electronic conductivity of the samples for SEM measurements. Figure 2d shows the typical HRTEM image and selected area electron diffraction (SAED) of the CuO spheres. The HRTEM image exhibits a regular lattice spacing of 0.23 nm, which agrees well with the (111) planes of monoclinic CuO, suggesting that the CuO nanoplates are single crystal and grow along the [111] direction. The electron diffraction pattern (inset of Figure 2d) recorded on CuO nanomicrospheres displays several concentric diffraction rings and some regular diffraction spots, indicating the polycrystalline nature of the spheres. Each individual CuO nanoplates is likely a single crystal, but X-ray beam for SAED experiments covers many nanoplates, resulting in polycrystalline features.

Images a and c in Figure 3 and Figure S5 in the Supporting Information present the typical SEM images of the as-prepared CuO-CNTs composites. The images clearly show that introducing CNTs does not change the shape and size of the CuO nanomicrospheres but results in a uniform distribution of CNTs into the CuO spheres and forms CuO-CNTs nanomicrospheres. From the SEM image of a broken sphere shown in Figure 3b and the inset there, it can be observed that the CNTs do not simply entangle on the surface of the CuO microspheres but are inserted into the inside of each microsphere. In order to investigate the effect of P123 on the final products, a control experiment with the absence of P123 was carried out. It was found that, in that case, only irregular CuO−CNT microparticles can be observed and the content of CNTs in the product is very low (see panels c and d in Figures S4 in the Supporting Information). The result indicates that P123 can not only promote the dispersion of CNTs but also increase the amount of CNTs in the final CuO−CNT composites. The formation process of the CuO−CNT nanomicrospheres is schematically shown in

(27) Yin, M.; Wu, C. K.; Lou, Y.; Burda, C.; Koberstein, J. T.; Zhu, Y.; O'Brien, S. *J. Am. Chem. Soc.* **2005**, *127*, 9506.

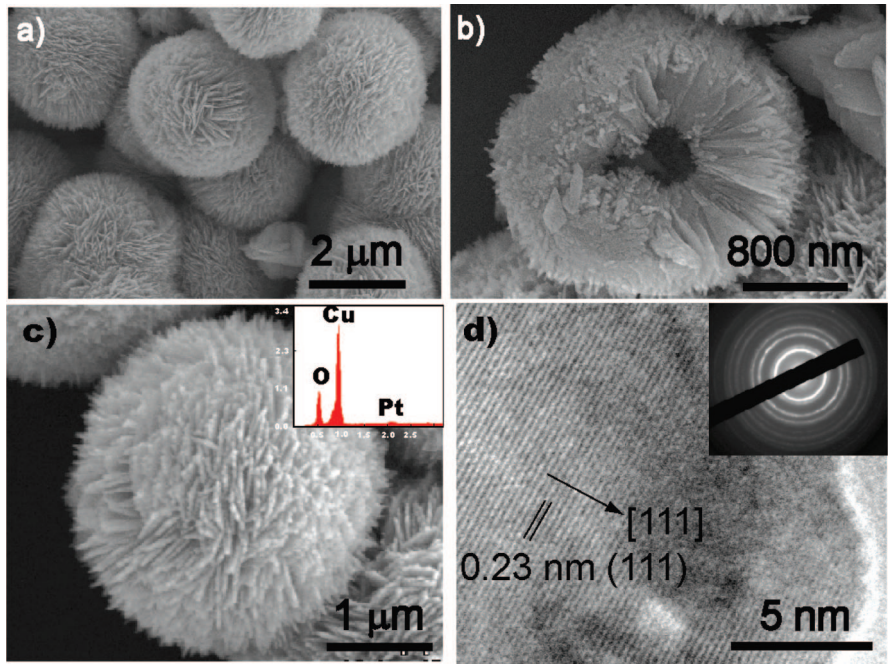

Figure 2. (a, c) SEM images of CuO nanomicrospheres, (b) crashed CuO nanomicrosphere, (d) HRTEM image of CuO nanomicrospheres.

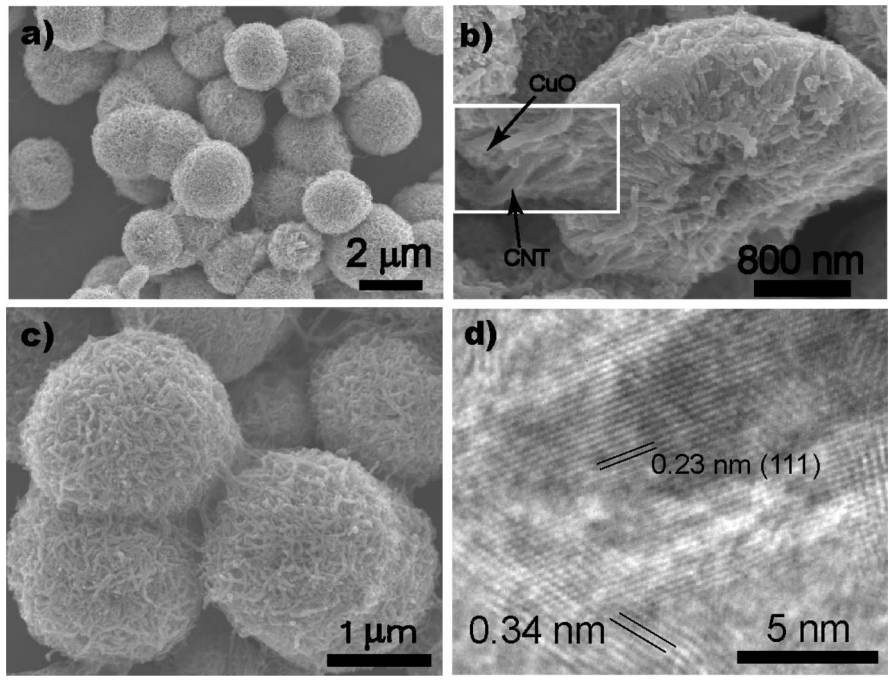

Figure 3. (a, c) SEM images of CuO−CNT nanomicrospheres and (b) crashed CuO−CNT nanomicrosphere, (d) HRTEM image of CuO−CNT nanomicrospheres. The inset in b shows the CuO crystals and the inserted CNTs.

Figure 4. During the synthesis, CuO does not nucleate on the surface of CNTs but grows under the direction of P123 micelles. As the CNTs were also uniformly dispersed around the spherical P123 micelles, many CNTs and CuO nanoplates were well mixed to form uniform CuO−CNT composite nanomicrospheres where many CNTs are inserted into the CuO microspheres with one end and the other end was extended out. If two micelles with growing CuO nanoplates were near enough, some CNTs might reach both of them with one end and result in two contacted CuO−CNT nanomicrospheres with CNTs bridges (see Figure 3c). Figure 3d shows a typical HRTEM image and SAED of a CuO−CNT composite. The HRTEM image shows the interface between the CuO and CNTs. The 0.34 nm spacing corresponds to the (002) crystalline planes of the MWCNTs, while the 0.23 nm lattice fringe arises from the (111) face distance of monoclinic CuO. These results further confirm the successful introduction of CNTs into CuO spheres.

As the MWCNTs used in our experiments have very high electronic conductivity, the successful introduction of CNTs into CuO spheres may enhance the electronic conductivities of the intra- and inter-CuO particles, which is favorable for use of CuO as an anode material for lithium-ion batteries. It was found that the overall electronic conductivity of the CuO-CNTs composites (∼0.1 S/cm) is enhanced by as much as 5

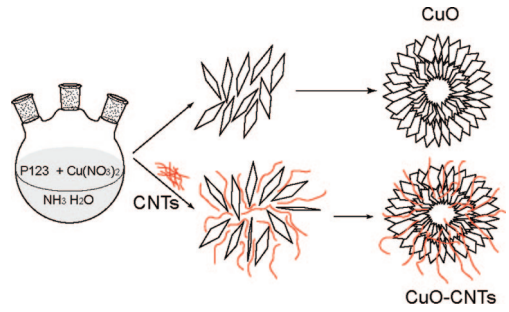

Figure 4. Schematic illustration for fabricating CuO and CuO−CNT nanomicrospheres.

orders of magnitude compared to that of the CuO spheres ($\sim 1 \times 10^{-6}$ S/cm).

To demonstrate the potential application of the present CuO−CNT nanomicrospheres with high electronic conductivity, we carried out a preliminary investigation into their electrochemical performance toward Li uptake−release compared with that of the CuO nanomicrospheres without CNTs. It was found that the first discharge/charge voltage profiles as well as the stabilized ones (see Figure 5) for CuO and CuO−CNTs are very similar, implying that the addition of CNTs to CuO does not change the electrochemical performance of the CuO nanomicrospheres. There are three pseudoplateaus (2.5−2.0, 1.35−1.25, and 1.0−0.02 V vs Li^+/Li, respectively) for the Li reaction with CuO, corresponding to the multistep electrochemical Li reaction process or additional sites for Li uptake, whereas there are no obvious potential plateaus for Li release from the crystal lattice of CuO.[28–30] Below 0.7 V, the potential tends to decrease gradually as the discharge depth increases. The behavior is similar to that described in the literature.[28,29] The electrochemical performance of pure CNTs was also studied for comparison. The results were also shown in Figure S6 in the Supporting Information. It was found that the CNTs used in our experiments have a reversible capacity of about 360 mA h g^{-1}, which indicates that the CNTs are an active materials toward Li uptake−release rather than inactive materials. So, the specific capacity of the CuO−CNTs composite was calculated on the basis of the whole mass. It is worth noting that the initial discharge capacity of the as-prepared CuO−CNTs is about 860 mA h g^{-1}, which is larger than the theoretical capacity of 670 mA h g^{-1} based on a maximum uptake of 2 Li per CuO, but it is much lower than that of the CuO spheres (ca. 970 mA h g^{-1}) and those reported in the literature, in which the discharge capacity much overexceeds the theoretical capacity.[28] Usually, the first discharge capacity of CuO considerably exceeds the nominal capacity and is ascribed to the electrolyte being reduced to form a solid electrolyte interphase (SEI) layer, the reduction of the adsorbed impurities on CuO surfaces, the initial formation of lithium oxide due to the presence of some residual OH^- groups in the surface of active CuO,

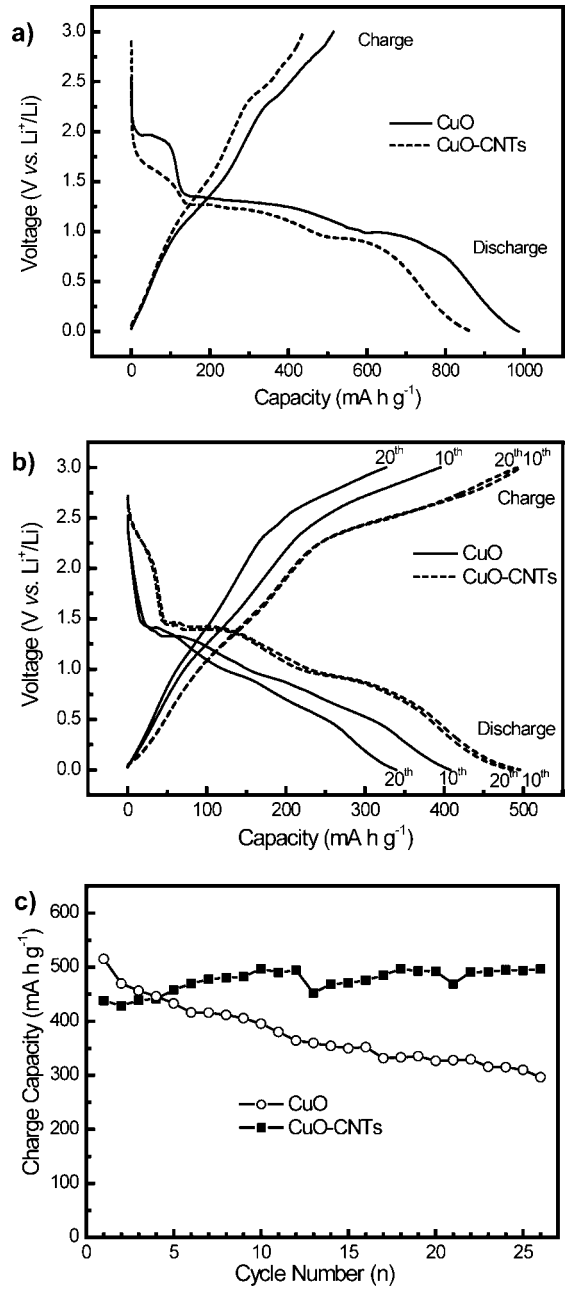

Figure 5. (a) First and (b) 10th and 20th discharge/charge voltage profiles of CuO and CuO−CNT nanomicrospheres cycled at a rate of *C*/10. (c) Variation in charge capacity versus cycle number for CuO and CuO−CNT nanomicrospheres at a rate of *C*/10.

and possibly interfacial lithium storage.[31] The relatively low overexceed capacity of the CuO−CNT spheres indicates that the decomposition of the electrolyte toward the formation of a SEI film on the CuO surface in the low potential region is less significant than that of the CuO spheres. This is a good phenomenon for CuO−CNTs as the anode material of lithium-ion batteries because it does not consume lots of Li ions supplied by the cathode materials.

Another excellent property of the CuO−CNT nanomicrospheres is the significantly enhanced cycling performance compared with the CuO nanomicrospheres. The results are shown in Figure 5c, in which a rate of *C*/10 (two lithium per formula unit in 10 h) has been employed. The first charge

(28) Gao, X. P.; Bao, J. L.; Pan, G. L.; Zhu, H. Y.; Huang, P. X.; Wu, F.; Song, D. Y. *J. Phys. Chem. B* **2004**, *108*, 5547.
(29) Morales, J.; Sanchez, L.; Martin, F.; Ramos-Barrado, J. R.; Sanchez, M. *Electrochim. Acta* **2004**, *49*, 4589.
(30) Grugeon, S.; Laruelle, S.; Herrera-Urbina, R.; Dupont, L.; Poizot, P.; Tarascon, J. M. *J. Electrochem. Soc.* **2001**, *148*, A285.
(31) Maier, J. *Nat. Mater.* **2005**, *4*, 805.

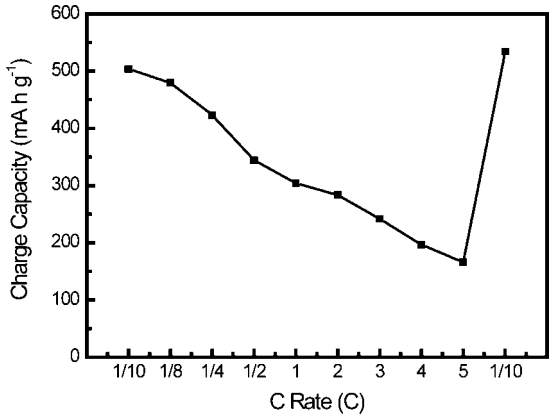

Figure 6. Rate performance of CuO−CNT nanomicrospheres.

capacity of CuO nanomicrospheres is 515 mA h g^{-1}. However, this value quickly decreases to 395 mA h g^{-1} after 10 cycles, 326 mA h g^{-1} after 20 cycles, and 296 mA h g^{-1} after 25 cycles, indicating poor capacity retention. In the case of the CuO−CNT nanomicrospheres, the specific charge capacity increases gradually during the initial several cycles, and then stabilizes at about 500 mA h g^{-1}, showing good retention of capacity on cycling. The rate capability of the CuO−CNT nanomicrospheres has also been investigated at room temperature. The results are shown in Figure 6 and Figure S7 in the Supporting Information. At a high rate of 5*C* (discharge/charge of all CuO within 12 min, i.e., 3350 mA g^{-1}), the specific charge capacity of CuO−CNTs is still 166 mA h g^{-1}, which is much larger than that of CuO (<100 mA h g^{-1}). The reversibility of CuO−CNTs is demonstrated by the fact that the capacity of about 500 mA h g^{-1} is regained if the rate is lowered to *C*/10. The results indicate that introducing CNTs into CuO is an effective way to improve both the cycling performance and rate performance of the composite material. The improvement is attributed to the following two factors. On one hand, the 3D network of CNTs can be considered as a 3D current collector network, which provides negligible diffusion times, and enhanced electronic conductivity, and hence is the key to the good rate (power) performance. On the other hand, in view of the large volume expansion of CuO during Li^+ uptake (CuO converts to Cu and Li_2O, about a 174% volume expansion), the 3D network of CNTs may also be considered as an elastic buffer to relieve the strain associated with the volume variations during Li uptake−release, and guarantees good cycling performance. Note that the Brunauer−Emmett−Teller (BET) specific surface areas of the CuO and the CuO−CNT samples are 4.11 and 25.98 m^2 g^{-1}, respectively. The result indicates that the introducing of CNTs also significantly enhances the specific surface area of the product, which may also contribute to the enhanced rate performance.

Conclusion

In summary, we have developed a simple solution method for large-scale synthesis of self-assembled CuO and CuO−CNT nanomicrospheres. Our results show that CuO itself has very poor cycling performance and rate performance because of its low electronic conductivity and large volume variations. After the addition of a 3D CNT network, the overall electronic conductivity of the CuO−CNT composite (∼0.1 S/cm) is enhanced by as much as 5 orders of magnitude compared to that of the CuO spheres (∼1 × 10^{-6} S/cm). The 3D network of CNTs acts as not only a 3D current collector network for both CuO nanomicrospheres and CuO nanoplates in individual sphere, but also as an elastic buffer to relieve the strain during Li uptake−release. As a result the capacity retention and rate capability of the CuO−CNT composite are significantly improved. The results here give clear evidence of the utility of dual functional CNT networks to improve the electrochemical performance of transition metal oxides as electrode materials for lithium-ion batteries. The strategy is simple, yet very effective, and because of its versatility could also be extended to other anode and cathode materials used in lithium-ion batteries.

Acknowledgment. The authors are grateful for the financial support from the National Natural Science Foundation of China (Grants 20603041, 20673121, 50730005, and 20701038), the National Key Project on Basic Research (Grants 2006CB806100 and 2006CB932100), and the Chinese Academy of Sciences. The authors thank Professor Chun-Li Bai for valuable advice, and Dr. Jie Shu for his help in the analysis and discussion of the experiments.

Supporting Information Available: IR (Figure S1) and XPS (Figure S2) spectra of CuO nanomicrospheres; large-scale SEM image of CuO sample (Figure S3); SEM images of the samples synthesized without P123 (Figure S4); large-scale SEM image of CuO−CNT sample (Figure S5); discharge/charge voltage profiles of MWCNTs (Figure S6); and CuO−CNTs nanomicrospheres cycled at different rates (Figure S7) (PDF). This material is available free of charge via the Internet at http://pubs.acs.org.

CM7033855